

Research Article

# Numerical solution of elliptic type of inverse problems by Pascal polynomial method

Muhammad Kareem<sup>1</sup>, Sakhi Zaman<sup>1</sup>, Ali Akgül<sup>2</sup>, Muhammad Nawaz Khan<sup>3,\*</sup>

<sup>1</sup>Department of Basic Sciences, University of Engineering and Technology, Peshawar, Pakistan.

<sup>2</sup>Department of Mathematics, Art and Science Faculty, Siirt University, Siirt, Turkey

<sup>3</sup>Mathematics in Applied Sciences and Engineering Research Group, Scientific Research Center, Al-Ayen University, Nasiriyah 64001, Iraq.

## ARTICLE INFO

### Article History

Received 16 Sep 2024

Revised 12 Nov 2024

Accepted 04 Dec 2024

Published 27 Dec 2024

### Keywords

Pascal polynomial method

Second-order inverse PDEs

Dirichlet boundary conditions

Neumann boundary conditions



## ABSTRACT

The Pascal polynomial approach is presented in this paper as an effective method for solving inverse partial differential equations (PDEs) of second order. Two different approaches are suggested. In the first method, Pascal polynomials are used to approximate the source term and the unknown dependent variable. A system of algebraic equations that can be solved is then produced by substituting these approximations and their derivatives into the governing equations and boundary conditions. By imposing a requirement that the source term satisfy Laplace's equation, the second approach reformulate the inverse problem as a direct one, which is subsequently solved via the Pascal polynomial method. We examine a number of benchmark problems to assess the suggested strategy, showing that it produces high accuracy when given accurate input data. Even though input data noise lowers accuracy, the numerical results are still reliable and acceptable. Despite its sensitivity to noise, these results demonstrate the potential of the Pascal polynomial approach for solving direct and inverse PDEs, especially when the input data is reliable.

## 1. INTRODUCTION

In many disciplines, including biology, physics, and engineering, inverse problems are common. Such problems arise from mathematical models of various social and physical phenomena. These models are based on fundamental principles of mathematics such as partial differential equations (PDEs), ordinary differential equations (ODEs), and integral equations (IEs). The solutions derived from these models enable predictions about the behavior of physical systems under different conditions, provided that all essential information is available. In the context of differential equations (DEs), such information may encompass initial and boundary conditions, source terms, coefficients associated with derivatives, and the geometry of the computational domain. When this data sufficiently characterizes the system, mathematical modeling becomes a feasible approach for analyzing physical phenomena.

Inverse heat source problems (IHSPs) find significant applications in engineering and biological sciences, such as detecting pollutants, identifying structural cracks, conducting geographical surveys, studying heat transfer, and analyzing electromagnetic phenomena [1, 2]. Often, the interior heat source term may be unavailable due to challenges in data collection, thereby giving rise to IHSPs [3]. Addressing the complexities associated with IHSPs, including the absence of source terms, typically requires additional information, such as boundary conditions, numerical data collected at specific points, or measurements within the accessible region of the boundary. These problems are inherently ill-posed, making their

\* Corresponding author. Email: [mnawaz77@gmail.com](mailto:mnawaz77@gmail.com)

numerical resolution challenging. Recovering the missing heat source term further complicates the process, and only a limited number of studies address these challenges [3, 4]. For instance, [4] used the method of fundamental solutions to address steady-state heat conduction problems involving a heat source term. The technique relied on the availability of both temperature and heat flux data on the same boundary to guarantee the uniqueness of the solution. To mitigate ill-conditioning in the coefficient matrix, a regularized solution was obtained using a truncated singular value decomposition (TSVD) method. Building upon this, [3] implemented a meshless generalized finite difference method (GFDM) for similar problems. Moreover, the method of fundamental solutions was explored in [5, 6], while [1] studied the inverse source problem for the Helmholtz equation, demonstrating solution uniqueness and local stability under specified boundary conditions and derivatives.

The GFDM has also been employed to tackle inverse biharmonic boundary value problems [7]. This investigation included adding noise to boundary conditions and imposing over-specified constraints on part of the boundary to assess method stability. Subsequently, [8] extended the GFDM to study a two-dimensional inverse Cauchy problem for a second-order linear PDE. Over-specified conditions on some boundary segments and noisy boundary data were used to illustrate the robustness of the numerical technique. For a comprehensive discussion on inverse Cauchy problems, readers are directed to [12–17], which detail various numerical methods for these problems.

This study addresses a steady-state heat conduction problem using the Pascal polynomial method. Consider a bounded domain  $\Omega$  where the IHSP is to be solved, with  $\partial\Omega$  representing its boundary. The equation that represents steady-state heat conduction is given as:

$$\Delta U_e(\mathbf{x}, \eta) = E_s(\mathbf{x}, \eta), \quad (\mathbf{x}, \eta) \in \Omega, \quad (1)$$

Here,  $\Delta$  signifies the Laplacian operator, while  $E_s(\mathbf{x}, \eta)$  and  $U_e(\mathbf{x}, \eta)$  represent the heat source term and the potential field, respectively. When the source term  $E_s(\mathbf{x}, \eta)$  is predefined, equation (1) is referred to as a direct problem. In such cases, solving the equation involves approximating only the function  $U_e(\mathbf{x}, \eta)$  using Pascal polynomial approximation. However, a key focus of this study is to treat the source term  $E_s(\mathbf{x}, \eta)$  as an unknown quantity. Under this assumption, equation (1) transitions into an inverse problem, where the goal is to determine the heat source  $E_s(\mathbf{x}, \eta)$ . It is important to highlight that such inverse problems often lack a unique solution [4]. Given the unknown nature of the heat source, we assume that the temperature and heat flux are specified along the accessible boundary portion  $\partial\Omega$  [3], as expressed by the following conditions:

$$\begin{aligned} U_e(\mathbf{x}, \eta) &= d_1(\mathbf{x}, \eta), \quad (\mathbf{x}, \eta) \in \partial\Omega, \\ \frac{\partial}{\partial \mathbf{n}} U_e(\mathbf{x}, \eta) &= d_2(\mathbf{x}, \eta), \quad (\mathbf{x}, \eta) \in \partial\Omega, \end{aligned} \quad (2)$$

Here,  $\mathbf{n}$  denotes the outward unit normal vector to the boundary  $\partial\Omega$ , and  $d_1(\mathbf{x}, \eta)$  and  $d_2(\mathbf{x}, \eta)$  are known values. To solve equation (1) along with the boundary conditions in (2), it is converted into a fourth-order elliptic partial differential equation. For example, if the source term  $E_s(\mathbf{x}, \eta)$  is harmonic, i.e., it satisfies  $\Delta E_s(\mathbf{x}, \eta) = 0$  or  $\nabla^2 E_s(\mathbf{x}, \eta) = 0$  within the domain  $\Omega$ , then equation (1) simplifies to a direct problem. By applying the  $\nabla^2$  operator to both sides of equation (1), we obtain:

$$\nabla^4 U_e(\mathbf{x}, \eta) := \frac{\partial^4}{\partial \mathbf{x}^4} U_e(\mathbf{x}, \eta) + 2 \frac{\partial^4}{\partial \mathbf{x}^2 \partial \eta^2} U_e(\mathbf{x}, \eta) + \frac{\partial^4}{\partial \eta^4} U_e(\mathbf{x}, \eta) = 0, \quad (\mathbf{x}, \eta) \in \Omega, \quad (3)$$

with the corresponding boundary conditions remaining as defined in equation (2). Additionally, equation (1) was solved by approximating both unknown functions using the Pascal polynomial method, which will be elaborated in the following sections.

## 2. PASCAL POLYNOMIAL COLLOCATION METHOD

This section applies the Pascal polynomial collocation method (CMBP) to solve the steady-state Inverse Heat Source Problems (IHSPs) given by (1), along with the associated boundary conditions (2).

In this approach, we approximate both the function of interest,  $U_e(\mathbf{x}, \eta)$ , and the source term,  $E_s(\mathbf{x}, \eta)$ , using the Pascal polynomial collocation method (CMBP). The numerical procedure of CMBP begins by considering the following:

$$U_e(x, y) = \sum_{\ell=1}^{\mathfrak{M}} \sum_{j=1}^{\ell} \lambda_{\ell j} x^{\ell-j} y^{j-1}, \quad (4)$$

and

$$E_s(x, y) = \sum_{\ell=1}^{\mathfrak{M}} \sum_{j=1}^{\ell} \beta_{\ell j} x^{\ell-j} y^{j-1}. \quad (5)$$

We proceed by computing the second derivatives of equation (1) with respect to the spatial variables  $x$  and  $y$ .

$$\begin{aligned} \frac{\partial^2}{\partial x^2} U_e(x, y) &= \sum_{\ell=1}^{\mathfrak{M}} \sum_{j=1}^{\ell} \lambda_{\ell j} (\ell - j)(\ell - j - 1) x^{\ell-j-2} y^{j-1}, \\ \frac{\partial^2}{\partial y^2} U_e(x, y) &= \sum_{\ell=1}^{\mathfrak{M}} \sum_{j=1}^{\ell} \lambda_{\ell j} (j - 1)(j - 2) x^{\ell-j} y^{j-3}. \end{aligned} \quad (6)$$

We now consider the following set of nodes:

$$\Omega_k = (x_{\iota_1}, y_{\zeta_1}) \in \Omega, \quad \iota_1 = \zeta_1 = 1, 2, 3, \dots, \mathfrak{M}, \text{ and } , \quad (7)$$

in the domain  $[a, b]^2$ , with the boundary nodes denoted as:

$$\Omega_b = (x_{\iota_2}, y_{\zeta_2}) \in \partial\Omega, \quad \iota_2 = \zeta_2 = 1, 2, 3, \dots, \mathfrak{M}_b, \text{ and } \quad (8)$$

Substituting equations (5) and (6) into (1) and applying the collocation method at the nodes within the domain  $\Omega_k$  (7), we derive a system of  $\mathfrak{M}^2$  equations with  $\mathfrak{M}(\mathfrak{M} + 1)$  unknowns.

$$\begin{aligned} \sum_{\ell=1}^{\mathfrak{M}} \sum_{j=1}^{\ell} \lambda_{\ell j} [(\ell - j)(\ell - j - 1) x_{\iota}^{\ell-j-2} y_{\zeta}^{j-1} + (j - 1)(j - 2) x_{\iota}^{\ell-j} y_{\zeta}^{j-3}] - \\ \sum_{\ell=1}^{\mathfrak{M}} \sum_{j=1}^{\ell} \beta_{\ell j} x_{\iota}^{\ell-j} y_{\zeta}^{j-1} = 0 \quad (x_{\iota}, y_{\zeta}) \in \Omega_k. \end{aligned} \quad (9)$$

The total number of nodes,  $\mathfrak{M}^2$ , significantly exceeds the count of unknowns,  $\mathfrak{M}(\mathfrak{M} + 1)$ , resulting in an overdetermined system. Additionally, the boundary conditions produce another set of equations, comprising  $2\mathfrak{M}_b$  equations that also involve  $\mathfrak{M}(\mathfrak{M} + 1)$  unknowns.

$$\begin{aligned}
\sum_{\ell=1}^{\mathfrak{M}} \sum_{j=1}^{\ell} \lambda_{\ell j} (\ell - j) a^{\ell-j-1} \eta_{\zeta_1}^{j-1} &= d_2(a, \eta_{\zeta_1}) \quad a \leq \eta_{\zeta_1} \leq b, \\
\sum_{\ell=1}^{\mathfrak{M}} \sum_{j=1}^{\ell} \lambda_{\ell j} (\ell - j) b^{\ell-j-1} \eta_{\zeta_1}^{j-1} &= d_2(b, \eta_{\zeta_1}) \quad a \leq \eta_{\zeta_1} \leq b, \\
\sum_{\ell=1}^{\mathfrak{M}} \sum_{j=1}^{\ell} \lambda_{\ell j} (j - 1) \bar{x}_{i_1}^{\ell-j} a^{j-2} &= d_2(\bar{x}_{i_1}, a), \quad a < \bar{x}_{i_1} < b, \\
\sum_{\ell=1}^{\mathfrak{M}} \sum_{j=1}^{\ell} \lambda_{\ell j} (j - 1) \bar{x}_{i_1}^{\ell-j} b^{j-2} &= d_2(\bar{x}_{i_1}, b), \quad a < \bar{x}_{i_1} < b. \\
\sum_{\ell=1}^{\mathfrak{M}} \sum_{j=1}^{\ell} \lambda_{\ell j} a^{\ell-j} \eta_{\zeta_1}^{j-1} &= d_1(a, \eta_{\zeta_1}), \quad a \leq \eta_{\zeta_1} \leq b, \\
\sum_{\ell=1}^{\mathfrak{M}} \sum_{j=1}^{\ell} \lambda_{\ell j} \bar{x}_{i_1}^{\ell-j} b^{j-1} &= d_1(\bar{x}_{i_1}, b), \quad a < \bar{x}_{i_1} < b, \\
\sum_{\ell=1}^{\mathfrak{M}} \sum_{j=1}^{\ell} \lambda_{\ell j} \bar{x}_{i_1}^{\ell-j} a^{j-1} &= d_1(\bar{x}_{i_1}, a), \quad a < \bar{x}_{i_1} < b, \\
\sum_{\ell=1}^{\mathfrak{M}} \sum_{j=1}^{\ell} \lambda_{\ell j} b^{\ell-j} \eta_{\zeta_1}^{j-1} &= d_1(b, \eta_{\zeta_1}), \quad a \leq \eta_{\zeta_1} \leq b,
\end{aligned} \tag{10}$$

The overdetermined systems of equations (9) and (10) can be solved together to determine the unknowns  $\lambda_{\ell j}$  and  $\beta_{\ell j}$ . Once these coefficients are determined, they are substituted into equations (4) and (5) to yield the approximated solutions. However, since the values of the source terms  $E_s(x, \eta)$  are not specified at the boundaries of the computational domain, this may lead to an imprecise approximation of  $E_s(x, \eta)$ . Conversely, the best numerical results for  $U_e(x, \eta)$  can be obtained, and its derivatives can be approximated more accurately. Thus, the source term  $E_s(x, \eta)$  is recovered from the following equation:

$$E_s(x, \eta) = \frac{\partial^2}{\partial x^2} U_e(x, \eta) + \frac{\partial^2}{\partial \eta^2} U_e(x, \eta), \quad (x, \eta) \in \Omega.$$

This approach addresses inverse problems directly, eliminating the requirement for any transformations.

## 2.1 Transformation of the Inverse Problem to the Direct Problem

This section outlines the procedure for converting the inverse heat conduction problem (1) into an equivalent direct problem. The approach assumes that the source follows the Laplace equation.

$$\frac{\partial^2}{\partial x^2} E_s(x, \eta) + \frac{\partial^2}{\partial \eta^2} E_s(x, \eta) = 0$$

By taking the Laplacian operator  $\nabla^2$  of both sides of equation (1), the direct problem is derived in the following manner:

$$\frac{\partial^4}{\partial x^4} U_e(x, \eta) + 2 \frac{\partial^4}{\partial x^2 \partial \eta^2} U_e(x, \eta) + \frac{\partial^4}{\partial \eta^4} U_e(x, \eta) = 0, \quad (x, \eta) \in \Omega, \tag{11}$$

The problem is subject to the boundary condition (2). By substituting the required derivatives into equation (11) and applying collocation at the nodes  $\Omega_k$ , a system of linear equations is obtained, consisting of  $\mathfrak{N}^2$  equations and  $\mathfrak{M}(\mathfrak{M} + 1)/2$  unknowns. A second system arises from the boundary conditions. These two systems are solved to determine the coefficients  $\lambda_{\ell j}$ , which are then used in equation (4) to obtain the numerical solution to the problem. Following this, the source term is recovered using equation (1). This process is referred to as CMBPT in this work.

### 3. NUMERICAL RESULTS

This section presents the numerical results obtained using the proposed CMBP and CMBPT methods, comparing them with existing results from the literature. Furthermore, an in-depth analysis of the stability of the proposed method is provided, focusing on its response to noise in the input data. In this study, noise is modeled within the exact boundary conditions using the equation:

$$B_n = (R_v\sigma + 1)b_n,$$

The random variable  $R_v$  is generated using the MATLAB 'rand' function, while  $b_n$  denotes the true boundary data. The noise level is represented by  $\sigma$ . To evaluate the effectiveness of the proposed methods, the following error norms are applied:

$$L_\infty = \max_{(x,y) \in \Omega} |U_e(x, y) - U_{app}|, \quad RMS = \sqrt{\frac{\sum_{k=1}^{\mathfrak{N}} (U_e(x_k, y_k) - U_{app})^2}{\sum_{k=1}^{\mathfrak{N}} U_e(x_k, y_k)^2}},$$

The exact solution at the  $k^{th}$  collocation point is denoted by  $U_e(x_k, y_k)$ , while  $U_{app}$  refers to the numerical approximation. The boundary is considered to be the entire boundary of the domain  $\Omega$ , unless stated otherwise. In both methods, the parameter  $\mathfrak{N}$  is assigned a value of 9, unless indicated otherwise.

### 4. EXAMPLES

In this section, various examples have been solved numerically to illustrate the robustness of the present method.

**Example 1.** In this example, we focus on the following equation [18]:

$$\begin{aligned} &\frac{\partial^4}{\partial x^4} U_e(x, y) + \frac{\partial^4}{\partial y^4} U_e(x, y) + 2\frac{\partial^4}{\partial x^2 \partial y^2} U_e(x, y) + 2y \sin(x) \frac{\partial}{\partial x} U_e(x, y) - \\ &y \cos(x) \frac{\partial}{\partial y} U_e(x, y) + xy U_e(x, y) = E_s(x, y), \quad (x, y) \in \Omega \end{aligned} \tag{12}$$

with the following Dirichlet and Laplace boundary conditions

$$\begin{aligned} U_e(x, y) &= g_1(x, y), \quad (x, y) \in \partial\Omega \\ \frac{\partial^2}{\partial x^2} U_e(x, y) + \frac{\partial^2}{\partial y^2} U_e(x, y) &= g_2(x, y), \quad (x, y) \in \partial\Omega, \end{aligned}$$

and the  $E_s(x, y)$  is given as:

$$\begin{aligned} E_s(x, y) &= x \cos(y) + y \sin(x) + xy (x \cos(y) + y \sin(x)) - \\ &y \cos(x) (\sin(x) - x \sin(y)) + 2y \sin(x) (\cos(y) + y \cos(x)) \end{aligned}$$

An Ellipse types of domain is considered, which can be defined by parametrically as:

$$\begin{aligned} x &= 3 \cos(\varphi)/2 \\ y &= \sin(\varphi). \end{aligned}$$

The arrangement of uniform collocation points in the specified domain for this example is shown in Figure (1). The results of CMBP are presented in Table (I). As observed in the earlier example, CMBP proves to be highly accurate in comparison with the numerical methods discussed in [18]. The RMS norm values for Multi-quadric and thin spline are  $4.0 \times 10^{-11}$ ,  $3.3 \times 10^{-11}$ , and  $1.0 \times 10^{-10}$ , while the method proposed in this study achieves  $2.8424 \times 10^{-17}$  with the same number of nodes. The table demonstrates that CMBP significantly outperforms the  $r^9$ ,  $r^{11}$ , and MQ methods in terms of RMS errors for sample sizes  $\mathfrak{N} = 200$  and  $\mathfrak{N} = 300$ . Furthermore, within the CMBP framework, an increase in the parameter  $M$  results in a reduction of RMS errors, indicating improved performance with higher  $M$  values. The subsequent examples will address solving inverse problems using CMBP and CMBPT.

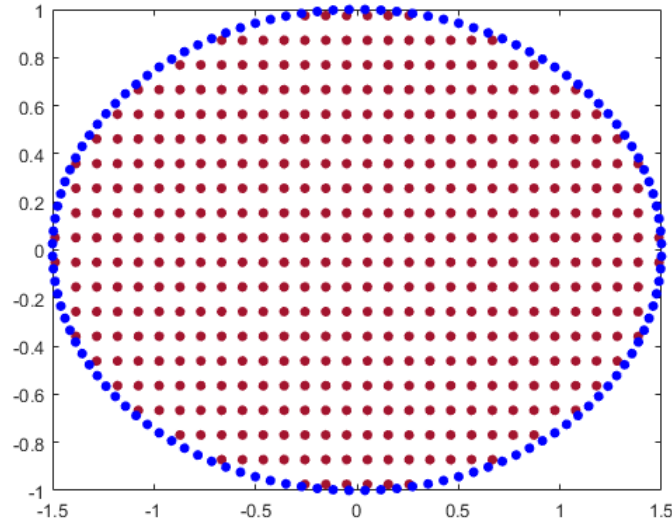


Fig. 1. Nodes arrangement for Example (1) in the domain.

TABLE I. Comparison of RMS error of CMBP against different methods.

$\mathfrak{N}$	RMS ( $r^9$ ) [18]	RMS ( $r^{11}$ ) [18]	RMS (MQ)[18]
200	$1.3 \times 10^{-10}$	$1.4 \times 10^{-10}$	$2.4 \times 10^{-10}$
300	$4.0 \times 10^{-11}$	$3.3 \times 10^{-11}$	$1.0 \times 10^{-10}$
CMBP			
$\mathfrak{N}$	RMS ( $M = 15$ )	RMS ( $M = 20$ )	RMS ( $M = 25$ )
200	$8.3553e - 13$	$1.9956e - 17$	$4.1368e - 17$
300	$7.2716e - 13$	$5.5688e - 17$	$3.3612e - 17$

**Example 2.** We examine the inverse heat conduction problem within a square region defined by  $[0, 6]^2$ . The source term  $E_s(x, y)$  and the exact solution  $U_e(x, y)$  are taken from [3].

$$U_e(x, y) = \frac{y^2 + x^2}{4}, \tag{13}$$

$$E_s(x, y) = 1. \tag{14}$$

The function  $E_s(x, y)$  is harmonic throughout the region  $\Omega$ . To address this problem, the CMBP and CMBPT techniques are applied. The distribution of nodes within the domain  $[0, 6]^2$  is illustrated in Figure (2).

The numerical results of Example (2) are presented in Figures (3), (4), and (5). Figure (3) shows the maximum error and relative error curves using CMBPT. In Figures (3)a and (4)a, exact data are used, while Figures (3)b and (4)b include 1% noisy data (i.e.,  $\sigma = 1\%$ ). The results indicate that both the CMBP and CMBPT methods perform well when exact input data are applied, with CMBP slightly outperforming CMBPT in Figures (3) and (4) for exact data. However, when noise are introduced into the input data, both methods yield less accurate results, but they remain suitable for solving inverse problems (IPs). As the noise in the boundary conditions is minimized, the outcomes of these methods converge toward the analytical solution. In summary, both methods can effectively recover the source terms  $E_s(x, y)$  and  $U_e(x, y)$  when the boundary conditions are exact.

According to [3], utilizing the generalized finite difference approach with 625 uniform nodes and the precise input data, the highest error norm for the same problem is  $8.26 \times 10^{-8}$ . However, [6], which likewise uses accurate input data, finds a maximum error norm of  $2.13 \times 10^{-7}$  for the same problem. As seen in Figures (3) and (4), the CMBP and CMBPT

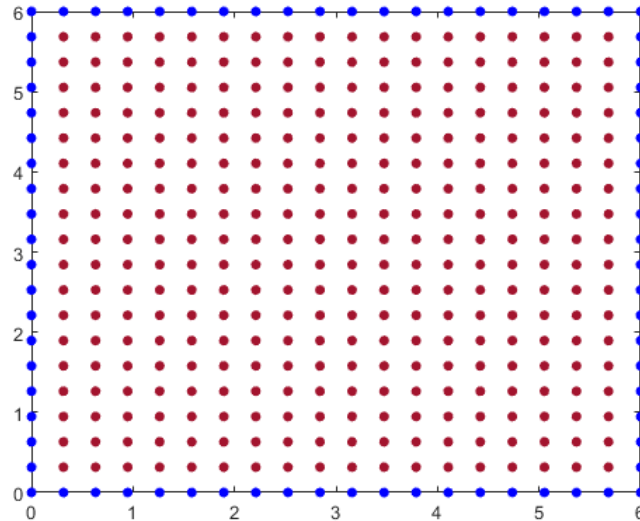


Fig. 2. Nodes arrangement of Example (2) in the domain.

approaches achieve lower maximum error norms with fewer uniform nodes in the domain, outperforming the techniques in [3, 4] in terms of accuracy.

Figure (5) shows the surface plots of the source term  $E_s(x, y)$  and the solution  $U_e(x, y)$ . Both the precise input data and input data with 1% additional noise are used in the study to evaluate the accuracy and performance of the suggested numerical algorithms.

## 5. CONCLUSION

This study presents the Pascal polynomial method for solving fourth-order partial differential equations (PDEs) and second-order inverse PDEs. For inverse problems, the source term  $E_s$  is considered unknown and satisfies the homogeneous Laplace equation. The second-order inverse problem is then reformulated as a fourth-order direct problem, which is numerically addressed through the Pascal polynomial method applied to the dependent variable  $U_e$ . The source term  $E_s$  is then determined by inserting the second-order derivatives back into the governing equation (1).

Furthermore, we approximate both  $U_e$  and  $E_s$  directly using Pascal polynomials, bypassing the need to convert the inverse problem into a direct one. This approach is advantageous when finding a suitable transformation is challenging. Using this technique, the coefficients involved in the approximation of  $E_s$  are determined. However, the lack of source term information at the accessible boundary results in poor numerical accuracy. To address this,  $E_s$  is retrieved from (1) by incorporating the necessary derivatives.

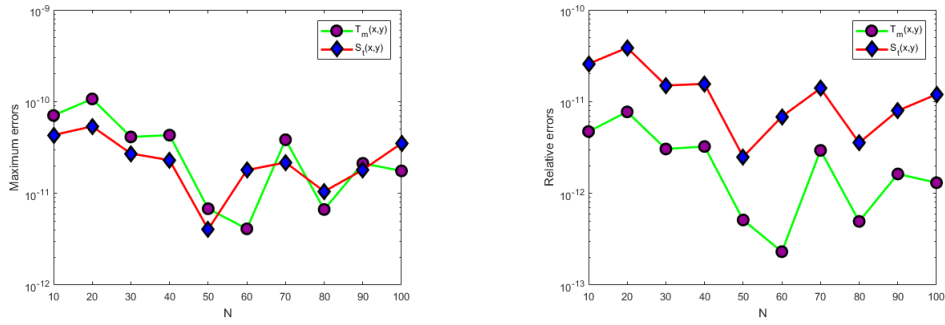
An in-depth examination of the Pascal polynomial method for solving inverse problems and fourth-order PDEs highlights several key insights into the performance of CMBP and CMBPT.

First, CMBP and CMBPT outperform many current numerical techniques in terms of accuracy and efficiency when given precise input data. These techniques use Pascal polynomials to produce better computational results, which are confirmed by theoretical analysis and benchmark examples.

However, noise in the input data affects how well they perform. In spite of this, CMBP and CMBPT achieve reliability that is consistent with accepted numerical standards while maintaining a competitive level of accuracy even in noisy environments.

In conclusion, CMBP and CMBPT are effective methods for resolving fourth-order PDEs and inverse problems, especially when used with precise input data. Even though noise lessens their efficacy, they are still as accurate as the industry's top techniques. They are useful for solving challenging mathematical problems because of their resilience.

(a) Accurate input information



(b) Input data with a noise level of 1%

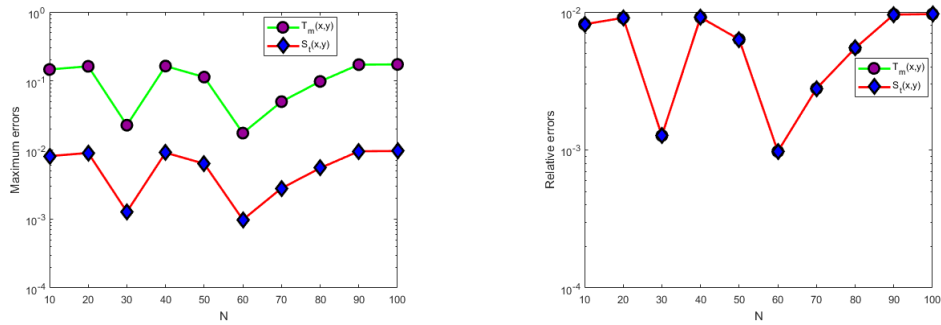
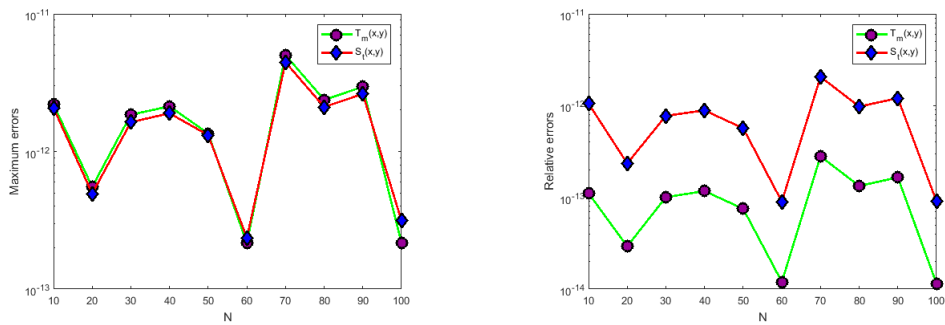


Fig. 3. Error analysis in relation to the number of nodes using CMBPT of Example (2).

(a) Accurate input information



(b) Input data with a noise level of 1%

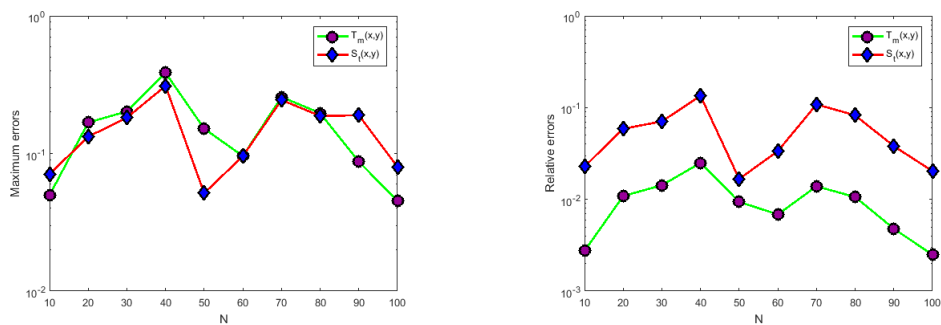
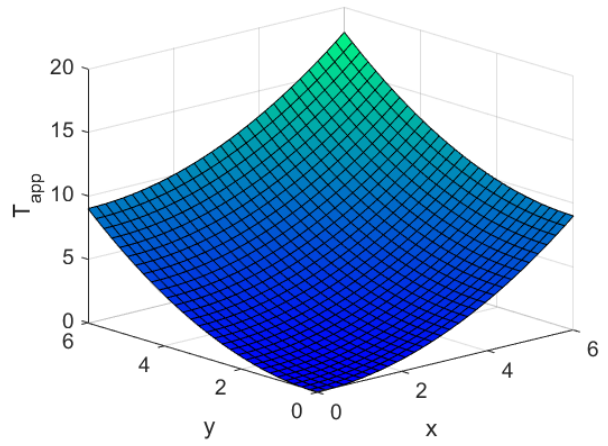
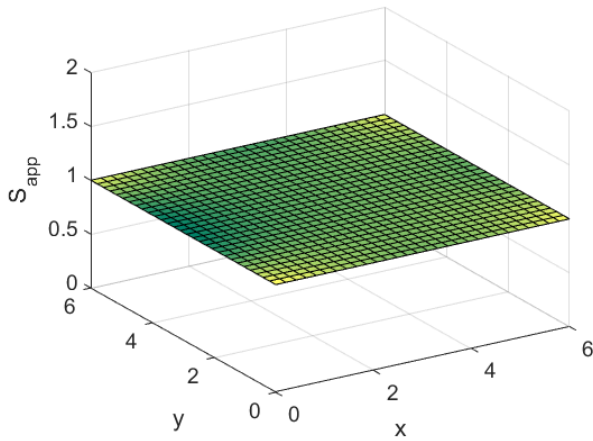


Fig. 4. Error analysis in relation to the number of nodes using CMBP of Example (2).

(a) Accurate input information



(b) Input data with a noise level of 1%

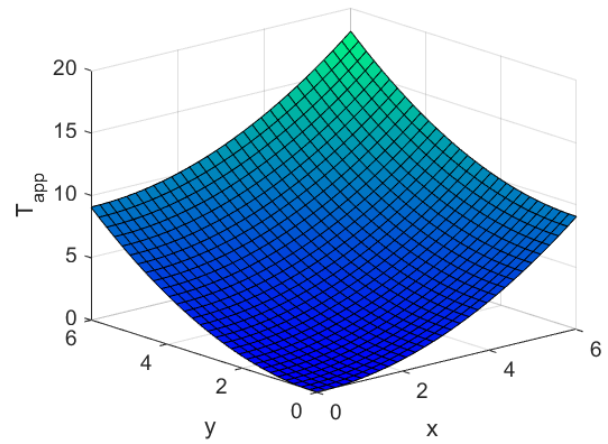
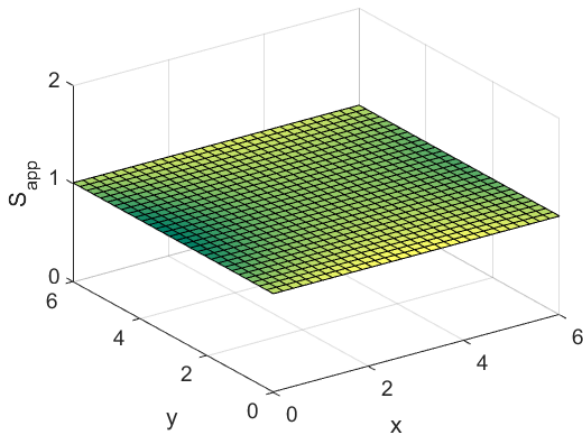


Fig. 5. Visual depictions of the outcomes through the CMBPT of Example (2) with  $M = 90$ .

## Conflicts of Interest

The authors declare no conflicts of interest.

## Funding

This research did not receive any specific grant from funding agencies in the public, commercial, or not-for-profit sectors.

## References

- [1] El Badia, A., & Nara, T. (2011). An inverse source problem for Helmholtz's equation from the Cauchy data with a single wave number. *Inverse Problems*, 27(10), 105001.
- [2] J. A. Devaney, A. E. Marengo & M. Li. (2007). Inverse source problem in nonhomogeneous background media, Handbook of mathematical economics. *SIAM Journal on Applied Mathematics*, 67(5), 1353–1378.
- [3] Gu, Y., Wang, L., Chen, W., Zhang, C., & He, X. (2017). Application of the meshless generalized finite difference method to inverse heat source problems. *International Journal of Heat and Mass Transfer*, 108, 721-729.
- [4] Jin, B., & Marin, L. (2007). The method of fundamental solutions for inverse source problems associated with the steady-state heat conduction. *International Journal for Numerical Methods in Engineering*, 69(8), 1570-1589.
- [5] Hon, Y. C., & Wei, T. (2004). A fundamental solution method for inverse heat conduction problem. *Engineering analysis with boundary elements*, 28(5), 489-495.
- [6] Hon, Y. C., & Wei, T. (2005). The method of fundamental solution for solving multidimensional inverse heat conduction problems. *CMES-Computer Modeling in Engineering and Sciences*, 7(2), 119-132.
- [7] Fan, C. M., Huang, Y. K., Li, P. W., & Chiu, C. L. (2014). Application of the generalized finite-difference method to inverse biharmonic boundary-value problems. *Numerical Heat Transfer, Part B: Fundamentals*, 65(2), 129-154.
- [8] Fan, C. M., Li, P. W., & Yeih, W. (2015). Generalized finite difference method for solving two-dimensional inverse Cauchy problems. *Inverse Problems in Science and Engineering*, 23(5), 737-759.
- [9] Khan, M. N., Siraj-ul-Islam, Hussain, I., Ahmad, I., & Ahmad, H. (2021). A local meshless method for the numerical solution of space-dependent inverse heat problems. *Mathematical Methods in the Applied Sciences*, 44(4), 3066-3079.
- [10] Ahsan, M., Lin, S., Ahmad, M., Nisar, M., Ahmad, I., Ahmed, H., & Liu, X. (2021). A Haar wavelet-based scheme for finding the control parameter in nonlinear inverse heat conduction equation. *Open Physics*, 19(1), 722-734.
- [11] Ahsan, M., Lei, W., Ahmad, M., Hussein, M. S., & Uddin, Z. (2022). A wavelet-based collocation technique to find the discontinuous heat source in inverse heat conduction problems. *Physica Scripta*, 97(12), 125208.
- [12] Fu, Z., Chen, W., & Zhang, C. (2012). Boundary particle method for Cauchy inhomogeneous potential problems. *Inverse problems in Science and Engineering*, 20(2), 189-207.
- [13] Zhou, D., & Wei, T. (2008). The method of fundamental solutions for solving a Cauchy problem of Laplace's equation in a multi-connected domain. *Inverse Problems in Science and Engineering*, 16(3), 389-411.
- [14] Lesnic, D., Elliott, L., & Ingham, D. B. (1997). A alternating boundary element method for solving Cauchy problems for the biharmonic equation. *Inverse Problems in Engineering*, 5(2), 145-168.
- [15] Chan, H. F., Fan, C. M., & Yeih, W. (2011). Solution of inverse boundary optimization problem by Trefftz method and exponentially convergent scalar homotopy algorithm. *Computers Materials and Continua*, 24(2), 125.
- [16] Karageorghis, A., Lesnic, D., & Marin, L. (2014). Regularized collocation Trefftz method for void detection in two-dimensional steady-state heat conduction problems. *Inverse Problems in Science and Engineering*, 22(3), 395-418.
- [17] El Badia, A. (2005). Inverse source problem in an anisotropic medium by boundary measurements. *Inverse Problems*, 21(5), 1487.
- [18] Reutskiy, S. Y. (2013). Method of particular solutions for solving PDEs of the second and fourth orders with variable coefficients. *Engineering Analysis with Boundary Elements*, 37(10), 1305-1310.